

Steric Retardation of S_N2 Reactions in the Gas Phase and SolutionGrigoriy Vayner,[†] K. N. Houk,^{*,†} William L. Jorgensen,^{*,‡} and John I. Brauman^{*,§}

Contribution from the Department of Chemistry and Biochemistry, University of California, Los Angeles, California 90095-1569; Department of Chemistry, Yale University, New Haven, Connecticut 06520-8107; and Department of Chemistry, Stanford University, Stanford, California 94305-5080

Received February 18, 2004; E-mail: houk@chem.ucla.edu

Abstract: The gas-phase S_N2 reactions of chloride with ethyl and neopentyl chlorides and their α -cyano derivatives have been explored with B3LYP, CBS-QB3, and PDDG/PM3 calculations. Calculations predict that the steric effect of the *tert*-butyl group raises the activation energy by about 6 kcal/mol relative to methyl in both cases. Solvent effects have been computed with QM/MM Monte Carlo simulations for DMSO, methanol, and water, as well as with a polarizable continuum model, CPCM. Solvents cause a large increase in the activation energies of these reactions but have a very small differential effect on the ethyl and neopentyl substrates and their cyano derivatives. The theoretical results contrast with previous conclusions that were based upon gas-phase rate measurements.

S_N2 reactions are a fundamental process of chemistry. In the gas phase, both experiment¹ and theory² indicate that the reactions involve double well potentials shown in Figure 1. Ion–molecule complexes are deep minima, and the energy of the transition structure is often lower than that of the separate reactants. The influence of solvation on the reaction profile is profound (Figure 2); in solution, the relatively localized charges of reactants and products are solvated more strongly than the ion–molecule complexes or transition states. The energy of activation for chloride attack on methyl chloride changes from 3 kcal/mol in the gas phase³ to above 20 kcal/mol in water.⁴

Steric effects have a major influence on the rates of S_N2 reactions. Ingold and Hughes found that S_N2 reactions of neopentyl bromides have 5–7 kcal/mol higher activation energies than ethyl bromides.⁵ Reactions of ethoxide with alkyl bromides in ethanol or halogen exchange in acetone show similar behavior.⁵ The explanation for the increased activation

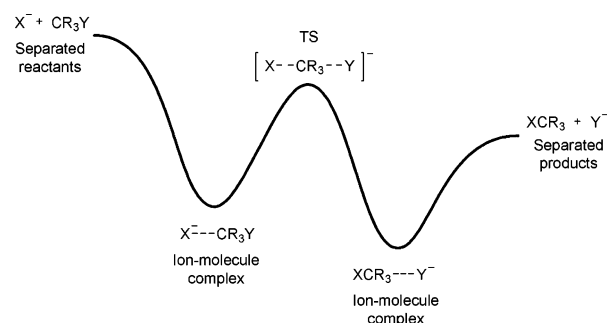


Figure 1. Generalized potential energy surface for S_N2 reactions in the gas phase.^{1,2}

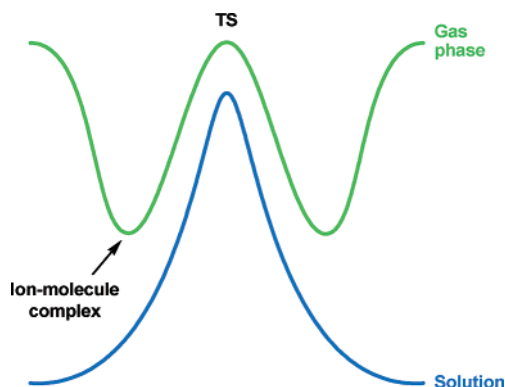


Figure 2. Contrast between gas (green) and solution (blue) phase potential energy surfaces for S_N2 reaction.^{1,2}

energy, common in organic textbooks and tacitly implied in most of the literature, refers to higher steric hindrance in the trigonal bipyramidal transition state; the larger substituents force the nucleophile and leaving group away from their ideal linear arrangement.^{6–8}

[†] University of California.

[‡] Yale University.

[§] Stanford University.

- (1) (a) Olmstead, W. N.; Brauman, J. I. *J. Am. Chem. Soc.* **1977**, *99*, 4219. (b) Barfknecht, T.; Dodd, J. A.; Salomon, K. E.; Tumas, W. E.; Brauman, J. I. *Pure Appl. Chem.* **1984**, *56*, 1809. (c) Caldweel, G.; Magnera, T. F.; Kebarle, P. *J. Am. Chem. Soc.* **1984**, *106*, 959. For a recent review, see: Laerdahl, J. K.; Uggerud, E. *Int. J. Mass Spectrom.* **2002**, *214*, 277.
- (2) (a) Berthier, G.; David, D.-J.; Veillard, A. *Theor. Chim. Acta* **1969**, *14*, 329. (b) Dedieu, A.; Veillard, A. *Chem. Phys. Lett.* **1970**, *5*, 328. (c) Dedieu, A.; Veillard, A. *J. Am. Chem. Soc.* **1972**, *94*, 6730. (d) Ritchie, C. D.; Chappel, G. A. *J. Am. Chem. Soc.* **1972**, *92*, 1819. (e) Duke, A. J.; Bader, R. F. W. *Chem. Phys. Lett.* **1971**, *10*, 631. (f) Gonzales, J. M.; Pak, C.; Cox, R. S.; Allen, W. D.; Schaefer, H. F.; Csaszar, A. G.; Tarczay, G. *Chem.—Eur. J.* **2003**, *9*, 2173.
- (3) Botchwina, P. *Theor. Chem. Acc.* **1998**, *99*, 426.
- (4) Based on the activation energies of unsymmetrical halogen exchange: McLennan, D. J. *Aust. J. Chem.* **1978**, *31*, 1897. Bathgate, R. H.; Moelwyn-Huges, E. A. *J. Chem. Soc.* **1959**, 2694.
- (5) (a) Dostrovski, I.; Hughes, E. D. *J. Chem. Soc.* **1946**, 157. (b) Dostrovski, I.; Hughes, E. D.; Ingold, C. K. *J. Chem. Soc.* **1946**, 173. (c) de la Mare, P. B. D.; Fowden, L.; Hughes, E. D.; Ingold, C. K.; Mackie, J. D. H. *J. Chem. Soc.* **1955**, 3200.

Recent gas-phase rate studies of chloride exchange in methyl- and *tert*-butyl-substituted chloroacetonitriles by Brauman et al. pointed to an additional mechanism for the rate effect.⁹ The measured gas-phase rate constants are in the ratio 6.25:1 in the gas phase, and the difference in activation energies derived from statistical RRKM rate theory is only 1.6 kcal/mol. The activation energy difference between these two reactions is expected to be close to the activation energy difference without the cyano groups; therefore, the steric effect in the gas phase is apparently substantially less than that in solution. The difference in activation energies suggests that solvation of the two transition states cannot be assumed to be identical. Monte Carlo simulations done at that time using TIP4P water solvation showed differential solvation of 4 kcal/mol for the two transition states (chloride plus methyl vs neopentyl chloride) and supported the view provided by experiment. Although classical steric effects were clearly observed in this and other systems, significant contributions of differential transition state solvation were required for a complete explanation.

To provide an independent theoretical estimate of energetics, the reactions have now been studied using several appropriate quantum mechanical methods, B3LYP/6-31G*,¹⁰ CBS-QB3,¹¹ both as implemented in Gaussian98,¹² and a new semiempirical method, PDDG/PM3.¹³ The last is a new method that is suitable for QM/MM studies in Monte Carlo simulations. CBS-QB3 is known to estimate heats of formation with average errors of ~1 kcal/mol for closed-shell molecules. Test calculations show that CBS-QB3 predictions of the barrier of different S_N2 reactions differ by about 0.5 kcal/mol from higher accuracy W1¹⁴ and W2 methods¹⁵ or CCSD(T) calculations with a very large basis set.³

The results of the CBS-QB3 calculations are represented in Tables 1 and 2, and Figures 3 and 4. The difference between the activation enthalpy (E + ZPE) barriers for ethyl (4.6 kcal/mol) and neopentyl (10.3 kcal/mol) chloride S_N2 reactions is 5.7 kcal/mol. The substitution of α -cyano groups lowers these barriers to -0.6 and 5.7 kcal/mol, respectively, leading to a difference of 6.3 kcal/mol; the cyano-substituted molecules are good models for ethyl and neopentyl chlorides. Nonetheless, the theoretical prediction of a 5.7 kcal/mol (or 6.3 kcal/mol for

Table 1. CBS-QB3 Energies (kcal/mol) of Ion–Molecule Complexes and TS Relative to Separated Reactants^a

reaction	ion–molecule complex	TS	retardation energy of <i>t</i> Bu vs Me
MeCl + Cl ⁻	-10.6 (-12.4)	2.0 (3.3)	
EtCl + Cl ⁻	-11.8 (-13.4)	4.6 (4.6)	
neopentylCl + Cl ⁻	-13.4 (-11.8)	10.3 (11.0)	5.7 (6.4)
MeCH(CN)Cl + Cl ⁻	-20.0 (-19.4)	-0.6 (2.6)	
<i>t</i> BuCH(CN)Cl + Cl ⁻	-21.7 (-21.7)	5.7 (9.3)	6.3 (6.7)

^a PDDG/PM3 energies are given in parentheses.

Table 2. CBS-QB3 Free Energies (kcal/mol) of Ion–Molecule Complexes and TS Relative to Separated Reactants

reaction	ion–molecule complex	TS	retardation energy of <i>t</i> Bu- vs Me-substituted system
MeCl + Cl ⁻	-5.2	8.0	
EtCl + Cl ⁻	-6.4	10.1	
neopentylCl + Cl ⁻	-7.1	17.3	7.2
MeCH(CN)Cl + Cl ⁻	-13.9	6.3	
<i>t</i> BuCH(CN)Cl + Cl ⁻	-14.9	12.6	6.3

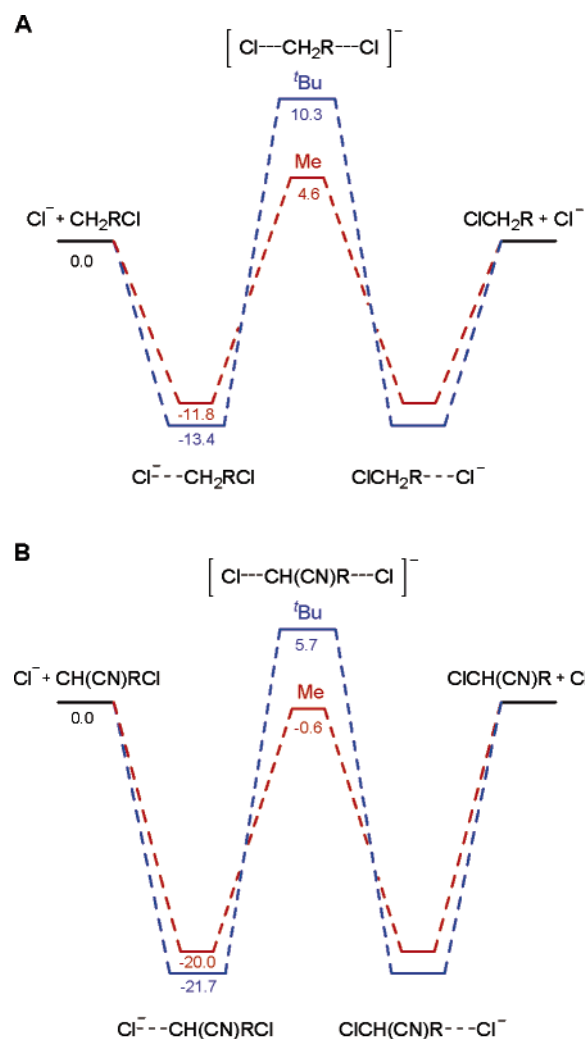


Figure 3. (A) Enthalpy profile of chloride exchange in ethyl (red, R = Me) and *neo*-pentyl (blue, R = *t*Bu) chlorides. (B) Enthalpy profile of chloride exchange in methyl (red, R = Me) and *tert*-butyl (blue, R = *t*Bu) substituted chloroacetonitriles.

cyano-substituted compounds) difference in activation energies of ethyl and neopentyl chloride reactions deviates significantly from the experimentally deduced value of 1.6 kcal/mol.⁹ In fact,

- Brown, W. H.; Foote C. S. *Organic Chemistry*, 3rd ed.; Saunders College Publishers: New York; p 283.
- Vollhardt, K. P. C.; Schore, N. E. *Organic Chemistry Structure and Function*, 4th ed.; Freeman and Co.: New York; p 235.
- March, J. *Advanced Organic Chemistry Reactions, Mechanisms, and Structure*, 4th ed.; John Wiley and Sons: New York; pp 275, 339.
- Regan, C. K.; Craig, S. L.; Brauman, J. I. *Science* **2002**, *296*, 2245.
- (a) Becke, A. D. *J. Chem. Phys.* **1993**, *98*, 1372. (b) Lee, C.; Yang, W.; Parr, R. G. *Phys. Rev. B* **1988**, *37*, 785.
- Montgomery, J. A., Jr.; Frisch, M. J.; Ochterski, J. W.; Petersson, G. A. *J. Chem. Phys.* **1999**, *110*, 2822.
- Frisch, M. J.; Trucks, G. W.; Schlegel, H. B.; Scuseria, G. E.; Robb, M. A.; Cheeseman, J. R.; Zakrzewski, V. G.; Montgomery, J. A., Jr.; Stratmann, R. E.; Burant, J. C.; Dapprich, S.; Millam, J. M.; Daniels, A. D.; Kudin, K. N.; Strain, M. C.; Farkas, O.; Tomasi, J.; Barone, V.; Cossi, M.; Cammi, R.; Mennucci, B.; Pomelli, C.; Adamo, C.; Clifford, S.; Ochterski, J.; Petersson, G. A.; Ayala, P. Y.; Cui, Q.; Morokuma, K.; Malick, D. K.; Rabuck, A. D.; Raghavachari, K.; Foresman, J. B.; Cioslowski, J.; Ortiz, J. V.; Stefanov, B. B.; Liu, G.; Liashenko, A.; Piskorz, P.; Komaromi, I.; Gomperts, R.; Martin, R. L.; Fox, D. J.; Keith, T.; Al-Laham, M. A.; Peng, C. Y.; Nanayakkara, A.; Gonzalez, C.; Challacombe, M.; Gill, P. M. W.; Johnson, B. G.; Chen, W.; Wong, M. W.; Andres, J. L.; Head-Gordon, M.; Replogle, E. S.; Pople, J. A. *Gaussian 98*, revision A.7; Gaussian, Inc.: Pittsburgh, PA, 1998.
- Repasky, M. P.; Chandrasekhar, J.; Jorgensen, W. L. *J. Comput. Chem.* **2002**, *23*, 1601. Tubert-Brohman, I.; Guimaraes, C. R. W.; Repasky, M. P.; Jorgensen, W. L. *J. Comput. Chem.* **2004**, *25*, 138.
- Martin, J. M. L.; De Oliveira, G. *J. Chem. Phys.* **1999**, *111*, 1843.
- Parthiban, S.; De Oliveira, G.; Martin, J. M. L. *J. Phys. Chem. A* **2001**, *105*, 895.

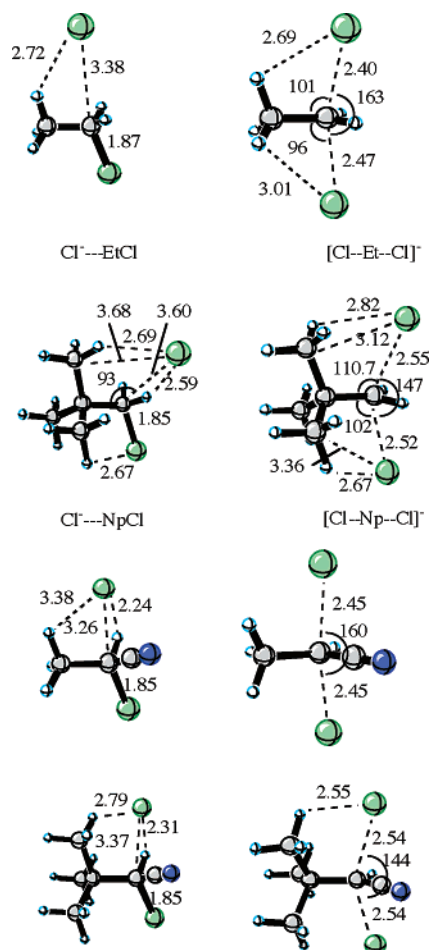


Figure 4. Geometries of ion-molecule complexes and TS for chloride exchange reactions in (A) ethyl and neopentyl chlorides and (B) methyl- and *t*Bu-substituted chloroacetonitriles. Partial bonds and nonbonded distances are shown.

the theoretical results are similar to the experimental values for related systems measured in various solvents (5–7 kcal/mol).⁵

The geometries from the B3LYP/6-311G(2d,d,p) used in the CBS-QB3 calculations are shown in Figure 4. In alkyl complexes and TSs, the nearest distance between chlorides and methyl hydrogens is ~ 2.7 – 2.8 Å, and introducing the CN group in the molecule shortens this distance to ~ 2.3 Å between Cl and HC(CN). The Cl–C–Cl angle is the expected 180° in the D_{3h} Cl–Me–Cl TS, becomes 163° in the ethyl TS, and is only 147° for neopentyl. These reduced angles maintain the 2.7 Å $H\cdots Cl^-$ nonbonded interaction. This angle deformation is the major cause of energy increase in the neopentyl TS versus the methyl or ethyl TS; when the $Cl^- + MeCl$ TS angle is constrained to 163° and 147° , the energy increases by 2.7 and 9.2 kcal/mol, respectively. The van der Waals repulsion between the chlorides and *t*-Bu group in the transition state distorts the Nuc–C–Nuc angle and increases the activation energy.

PDDG/PM3 optimizations were also carried for these processes. The energetics are given in parentheses in Table 1. In all cases, the two C–Cl distances were found to be essentially the same in the transition structures. The key geometrical parameters are summarized and compared to CBS-QB3 in Table 3. The main points are the following: (1) As with B3LYP geometries, replacement of an ethyl group in the substrates by neopentyl is found to increase the overall activation barriers by

Table 3. Gas-Phase B3LYP/6-311G(2d,d,p) Geometries (C–Cl Distances and Cl–C–Cl Angles)^{a,b}

reaction		ion-dipole complex	TS
MeCl + Cl [−]	$r(C\cdots Cl)$	3.146 (2.953)	2.364 (2.246)
	$\angle(CICCl)$	180 (180)	180 (180)
EtCl + Cl [−]	$r(C\cdots Cl)$	3.376 (3.093)	2.436 (2.289)
	$\angle(CICCl)$	165 (171)	163 (170)
neopentylCl + Cl [−]	$r(C\cdots Cl)$	3.595 (3.169)	2.53 (2.333)
	$\angle(CICCl)$	123 (155)	147 (153)
MeCH(CN)Cl + Cl [−]	$r(C\cdots Cl)$	3.263 (3.244)	2.448 (2.258)
	$\angle(CICCl)$	118 (126)	161 (170)
<i>t</i> BuCH(CN)Cl + Cl [−]	$r(C\cdots Cl)$	3.373 (3.345)	2.542 (2.286)
	$\angle(CICCl)$	114 (120)	144 (155)

^a PDDG/PM3 values are given in parentheses. ^b Distances in Å, angles in deg.

ca. 6 kcal/mol, while introduction of a cyano group lowers the barriers by 2 kcal/mol with PDDG/PM3 or 5 kcal/mol with CBS-QB3. (2) Variations in the C–Cl distances and Cl–C–Cl angles parallel those formed by B3LYP (Table 3). Thus, the C–Cl distances increase by ca. 0.04 Å (0.07 Å at the B3LYP level) in progressing from methyl to ethyl derivatives and by a similar amount from ethyl to neopentyl.

The effects of solvation on these barriers were explored both with continuum models and with full Monte Carlo simulations including explicit solvent. Free-energy perturbation (FEP) calculations were also carried out for the reactions of chloride ion with ethyl chloride and neopentyl chloride in DMSO, methanol, and water as solvents. The procedure was essentially the same as recently applied to Diels–Alder reactions¹⁶ and Claisen rearrangements.^{17–19} In brief, mixed quantum and molecular mechanics (QM/MM) calculations were carried out. The reacting system was treated with PDDG/PM3, while the solvent molecules were represented with the united-atom OPLS force field for the nonaqueous solvents and with the TIP4P water model. The solute–solvent interactions are represented by Coulomb and Lennard–Jones potentials. For the solute atoms, standard OPLS-AA Lennard–Jones parameters were adopted, and unscaled partial charges were used as obtained from the CM3 charge model²⁰ and the PDDG/PM3 wave functions. The statistical sampling for the FEP calculations was performed with Metropolis Monte Carlo simulations at 25 °C and 1 atm. Rectangular periodic cells were used; the systems consisted of the reactants plus 395 solvent molecules for the nonaqueous solvents or 740 molecules for water.

In the first set of FEP calculations, the transition structures were located by mapping the free energy as a function of the two C–Cl distances and the Cl–C–Cl angle in increments of 0.01 Å and 1° . The free-energy maps are flat within 0.1 kcal/mol for C–Cl lengths within 0.03 Å and Cl–C–Cl angles within 3° of the values reported here for the transition structures (Table 4). Each simulation consisted of 2.5 M configurations of equilibration followed by 4 M configurations of averaging in the nonaqueous solvents or 5 M in water. All degrees of freedom of reactants were sampled except for the scanned

(16) Chandrasekhar, J.; Shariffskul, S.; Jorgensen, W. L. *J. Phys. Chem. B* **2002**, *106*, 8078.

(17) Kaminski, G. A.; Jorgensen, W. L. *J. Phys. Chem. B* **1998**, *102*, 1787.

(18) Repasky, M. P.; Guimaraes, C. R. W.; Chandrasekhar, J.; Tirado-Rives, J.; Jorgensen, W. L. *J. Am. Chem. Soc.* **2003**, *125*, 6663.

(19) Guimaraes, C. R. W.; Repasky, M. P.; Chandrasekhar, J.; Tirado-Rives, J.; Jorgensen, W. L. *J. Am. Chem. Soc.* **2003**, *125*, 6892.

(20) Thompson, J. D.; Cramer, C. J.; Truhlar, D. G. *J. Comput. Chem.* **2003**, *24*, 1291.

Table 4. MC/FEP Results for S_N2 Reactions in Solution at 25 °C

RCl	solvent	TS: $r(\text{C}\cdots\text{Cl})$	TS: $\angle(\text{ClCCl})$	TS: $q(\text{Cl})$	ΔG^\ddagger
NpCl	DMSO	2.360	146	-0.83	23.9
EtCl	DMSO	2.305	168	-0.83	17.0
NpCl-EtCl		0.055	-22	0	6.9
NpCl	MeOH	2.430	147	-0.85	30.4
EtCl	MeOH	2.390	167	-0.85	24.8
NpCl-EtCl		0.040	-20	0	5.6
NpCl	H ₂ O	2.510	144	-0.86	30.4
EtCl	H ₂ O	2.470	166	-0.87	23.9
NpCl-EtCl		0.040	-22	0.01	6.5

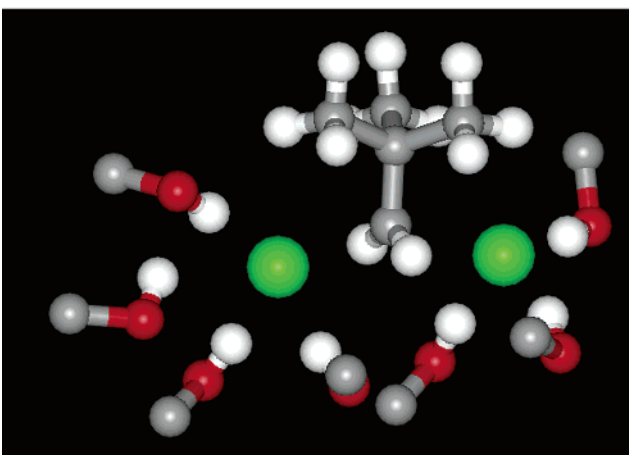
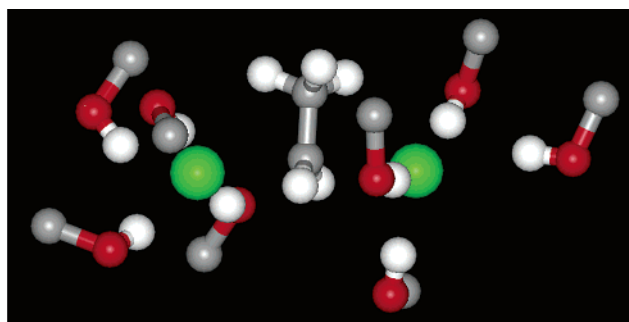
variables, while sampling of the internally rigid solvent molecules involved only their total translations and rotations.

Subsequently, FEP calculations were performed to obtain the free energies of activation by driving the transition structures to the reactant geometries at a $\text{Cl}^- \cdots \text{C}$ separation of 5.5 Å. FEP calculations were also carried out for each alkyl halide with chloride ion, and the free-energy profiles were confirmed to be flat beyond 5 Å. For the transition structure to reactant FEP calculations, the values for the C-Cl distances and Cl-C-Cl angles at the transition structures were fixed at the optimized values (Table 3), the covalent C-Cl distance for the reactant was fixed at the consensus value of 1.77 Å, and the chlorines and carbons C1 and C2 of the alkyl fragment were kept coplanar. All remaining degrees of freedom were sampled. Seemingly simple use of one C-Cl distance as the reaction coordinate does not lead to sampling of transition-state like structures at C-Cl separations in the vicinity of the saddle point; the other C-Cl distance prefers to remain near 1.8 Å. A viable alternative is to follow a gas-phase reaction path and then map off it to locate the stationary points in solution.^{18,19} For each system, results for 100 FEP windows were obtained through 50 separate MC simulations using double-wide sampling; the change in the $\text{Cl}^- \cdots \text{C}$ distance between windows was ca. 0.03 Å. Each MC simulation again covered a total of 6.5 or 7 M configurations. An attempt to move the solute was made every 100 configurations and requires computing the new QM energy for the solute and its two perturbed forms. Thus, the total number of PDDG/PM3 single-point calculations executed for each reaction was ca. 10 million. All calculations were carried out with the BOSS program.²¹ Only a single job submission is needed to compute a free-energy profile; the required computation times were ca. 1 and 2 days for each 100-window series of FEP calculations for the ethyl and neopentyl cases, respectively, on a 2.4 GHz Xeon processor running Linux.

Snapshots from the MC simulations are shown in Figure 5. The statistical uncertainties from the batch means procedure for the free-energy changes were 0.005–0.02 kcal/mol in each window. Thus, the overall uncertainties in the computed free energies of activation, ΔG^\ddagger , are below 0.2 kcal/mol ($0.02^2 \times 100$)^{1/2}. The computed ΔG^\ddagger values include a cratic correction of 1.9 kcal/mol to correspond to 1 M standard states.²² In DMSO, the predicted free energies of activation are 17.0 and 23.9 kcal/mol for the reactions with ethyl and neopentyl chloride, while the corresponding results are 24.8 and 30.4 kcal/mol in methanol and 23.9 and 30.4 kcal/mol in water.

(21) Jorgensen, W. L. *BOSS 4.5*; Yale University: New Haven, 2003.

(22) (a) Murphy, K. P.; Xie, D.; Thompson, K. S.; Amsel, L. M.; Freire, E. *Proteins: Struct., Funct., Genet.* **1994**, *18*, 63. (b) Hermans, J.; Wang, L. *J. Am. Chem. Soc.* **1997**, *119*, 2707.

**Figure 5.** Snapshots from molecular dynamics of solvated TS for chloride exchange in ethyl and neopentyl chlorides in methanol solution.**Table 5.** Activation Free Energies of Reactions in DMSO, MeOH, and Water Solutions^a

reaction	ΔG^\ddagger			retardation energy of $t\text{Bu}$ vs Me		
	DMSO	MeOH	H ₂ O	DMSO	MeOH	H ₂ O
MeCl + Cl^-	32.0	34.9	35.3			
EtCl + Cl^-	35.4	38.0	38.4			
neopentylCl + Cl^-	44.1	47.1	47.6	8.7	9.1	9.3
MeCH(CN)Cl + Cl^-	35.8	39.8	40.5			
$t\text{BuCH(CN)Cl}$ + Cl^-	42.1	46.5	46.9	6.3	6.7	6.4

^a CBS-QB3 gas-phase free energies were corrected by B3LYP/6-31G*/CPCM (geometries optimized in solution) solvation free energies.

CPCM²³ continuum solvation optimizations were also performed, and the results for different polar solvents (DMSO, methanol and water) are shown in Table 5. The free energy of the TS relative to reactants rises by 24–27, 25–28, and 27–30 kcal/mol in the cases of the methyl, ethyl, and the neopentyl TS, respectively. These calculations predict that the activation energy difference increases in polar solvents by 1–1.5 kcal/mol from methyl to ethyl chloride and by 1.5–2 kcal/mol from ethyl to neopentyl chloride, that is, about a fourth of the theoretical gas phase energy difference between activation energies of ethyl and neopentyl chlorides. This occurs because the ion-induced dipole interaction between the partially negative chloride atoms and $t\text{-Bu}$ group is smaller in polar media than in gas phase. This effect is found even in the ion–molecule complexes; the energy of the neopentyl complex (gas-phase geometry) is increased in water by 3.8 kcal more than the energy of the ethyl complex. The geometry changes of transition

(23) (a) Barone, V.; Cossi, M. *J. Phys. Chem. A* **1998**, *102*, 1995. (b) Barone, B.; Cossi, M.; Tomasi, J. *J. Comput. Chem.* **1998**, *19*, 404.

structures during solution phase optimization in the CPCM model are small; the main difference between gas and solution phase geometries is an increase of C–Cl distance by 0.04, 0.06, and 0.08 Å in DMSO, MeOH, and water solutions, respectively. The rest of the changes in neopentyl and all changes in ethyl TS geometry from gas to solution phase are insignificant (less than 0.01 Å and 1°). The MC computed solution-phase barriers are in the expected range based on experimental data for related systems,^{24–26} although experimental data on the present degenerate exchange reactions have not been reported. All of the computational methods provide good agreement when experimental data are available. As an example, the experimental ΔG^\ddagger for the reaction of chloride ion with ethyl iodide in methanol at 30 °C is 25.8 kcal/mol.²⁶ Naturally, the barriers in polar solvents are much higher than in the gas phase owing to the better solvation of the chloride ion than the more charge-delocalized transition structures.²⁷ Observed rate ratios for S_N2 reactions in different solvents depend on the leaving group and nucleophile; for reactions of azide ion with octyl chloride,²⁸ the rate ratio is 177 ($\Delta\Delta G^\ddagger = 3.4$ kcal/mol) for DMSO vs MeOH at 60 °C and, for chloride ion with ethyl iodide, $\Delta\Delta G^\ddagger = 5.4$ kcal/mol for acetonitrile vs methanol at 30 °C.²⁸ For the reaction of methyl iodide with chloride ion, the observed rate ratio is 4×10^4 to 1 for acetonitrile to methanol ($\Delta\Delta G^\ddagger = 5.8$ kcal/mol), and in general, rates of S_N2 reactions in methanol and water are usually within a factor of 2.²⁹ The corresponding differences for the present reactions can be expected to be greater, since the more charge-localized chloride ion is both nucleophile and leaving group. Consequently, the computed differences of 6–8 kcal/mol for the dipolar aprotic vs protic solvents in Table 4 are reasonable. The predicted ethyl to neopentyl differences of 6.9, 5.6, and 6.5 kcal/mol are also in the correct order and correspond closely in magnitude to the often quoted rate ratios of 10^5 (6–7 kcal/mol) for this pair.^{25,30}

The C–Cl distances in the transition structures do increase in progressing to more polar media in order to benefit from better solvation of the chlorides, which have charges of ca. $-0.8 e$ (Table 4). Specifically, the bond-length differences amount to 0.1 Å in going from the gas phase to methanol solution and by nearly 0.2 Å in progressing to water (Tables 3 and 4). The Cl–C–Cl angles in the transition structures are also pinched in by 2–3° and 6–9° for the ethyl and neopentyl cases, respectively, in solution versus the gas phase to allow less encumbered solvation. Overall, the structural differences between the two cases, 0.04 Å for the C–Cl length and 17° for the Cl–C–Cl angle in the gas phase (Table 3), are changed little by solvation (Table 4). Counts of hydrogen bonds for the transition states can also be readily obtained, since the Cl...HOR radial distribution functions show sharp minima at 2.5-Å separation. From integration to this cutoff, the number of hydrogen bonds with methanol molecules is 6.6 and 7.0 for the

ethyl and neopentyl chloride transition states, respectively. In water, the corresponding numbers are 8.5 and 9.1. Similarly, in comparing the gas-phase activation energies and the results in solution, the gas-phase difference of 6.4 kcal/mol is well maintained (Table 4). There is no indication of a substantial steric solvation penalty for the neopentyl system. The present results support a view wherein the steric penalty for neopentyl chloride as electrophile is largely carried over from the gas phase into solution.

It is possible that the discrepancy between theory and the gas-phase experiment may reflect nonstatistical behavior in the gas-phase reactions. Some halide exchanges in methyl halides proceed with significant TS recrossing.³¹ Transition state theory (TST) and RRKM theory may not give accurate activation barriers from the reaction rate and vice versa. However other studies suggested that substituents such as cyano groups eliminate nonstatistical effects.³² Moreover, nonstatistical behavior of this type is likely to produce slower, rather than faster, rates. In general, accurate measurement of slow reactions is difficult, due to the intervention of other processes, which produce the same product (chloride ion). If fast, they will give an apparent rate faster than the one under consideration. Although great pains were taken to purify the compounds, and the rates were reproduced many times, it is still possible that some other process was also occurring. On the other hand, CBS methods are well-known for high precision energy calculations of gas-phase reactions including steric effects. When the difficulties of an indirect experimental measurement of activation barriers and the high accuracy of the CBS-QB3 method are taken into account, it is most likely that the retardation of S_N2 reactions due to bulky substituents is only weakly dependent on the solvent system.

In conclusion, the activation energies for S_N2 reactions varying in steric effects were computed for the gas phase and for polar solvents. CBS-QB3 calculations predict the gas-phase steric effect to be similar to experimental values for aqueous solution. Contrary to the reported experiment, calculations suggest that the activation energy difference is mostly of steric origin and is similar in gas phase and different solvents. Intuitively, nonidentical S_N2 transition states must be solvated to different extents, but classical steric effects quantitatively describe the rate effects to a greater extent than originally concluded. Additional studies may explain the origin of this discrepancy.

Acknowledgment. This research was stimulated by an interesting conversation with George Whitesides. We are grateful to the National Science Foundation (CHE-0240203 and CHE-0130996) for financial support of this research. J.I.B. thanks C. Regan and S. Craig for a critical reading and helpful discussions. We thank Fernando Clemente for expert assistance with graphics.

Supporting Information Available: The Cartesian coordinates for the ion–molecule complexes and transition states. This material is available free of charge via the Internet at <http://pubs.acs.org>.

JA049070M

- (24) Albery, W. J.; Kreevoy, M. M. *Adv. Phys. Org. Chem.* **1978**, *16*, 87.
(25) DeTar, D.; McMullen, D. F.; Luthra, N. P. *J. Am. Chem. Soc.* **1978**, *100*, 2484.
(26) Kondo, Y.; Siotani, H.; Kusabayashi, S. *J. Chem. Soc., Faraday Trans. 1* **1984**, *80*, 2145.
(27) Chandrasekhar, J.; Smith, S. F.; Jorgensen, W. L. *J. Am. Chem. Soc.* **1985**, *107*, 154.
(28) Landini, D.; Maia, A.; Montanari, F.; Rolla, F. *J. Org. Chem.* **1983**, *48*, 3774.
(29) Alexander, R.; Ko, E. C. F.; Parker, A. J.; Broxton, T. J. *J. Am. Chem. Soc.* **1968**, *90*, 5049.
(30) Smith, M. B.; March, J. *March's Advanced Organic Chemistry*, 5th ed.; Wiley: New York, 2001; p 432.

- (31) Hase, W. L. *Science* **1994**, *266*, 998.
(32) Craig, S. L.; Brauman, J. I. *Science* **1997**, *276*, 1536. Viggiano, A. A.; Morris, R. A.; Su, T.; Wladkowski, B. D.; Craig, S. L.; Zhong, M.; Brauman, J. I. *J. Am. Chem. Soc.* **1994**, *116*, 2213.